ELECTRONICS AND ELECTRICAL ENGINEERING
ISSN 1392 – 1215 2007. No. 5(77)
ELEKTRONIKA IR ELEKTROTECHNIKA

T191 HIGH FREQUENCY TECHNOLOGY, MICROWAVES
AUKŠTŲJŲ DAŽNIŲ TECHNOLOGIJA, MIKROBANGOS

Model of the Coupled Transmission Lines with a non-uniform Dielectric

V. Urbanavičius, Š. Mikučionis, R. Martavičius
Department of Electronic Systems, Vilnius Gediminas Technical University,
Naugarduko st. 41-422, LT-03227 Vilnius, Lithuania, tel.: +370 5 2744756, e-mail: vytautas.urbanavicius@el.vtu.lt

Introduction

Parallel coupled microstrip transmission lines in inhomogeneous media have found use in microwave circuits as filters [1], couplers [2], phase shifters [3], etc. Quasi-TEM analysis of such structures reveals that multiple phase velocities as well as characteristic impedances are supported and must be considered for accurate prediction and understanding of circuit behavior [4]–[7].

In general, a transmission line which consists of $n+1$ conductors in an inhomogeneous dielectric and in which one conductor is taken as ground, supports n distinct "normal" quasi-TEM modes, each with distinct phase velocity and with distinct characteristic impedance for each line [6]. The case of a homogeneous dielectric represents a sort of symmetry in which the quasi-TEM modes become true-TEM modes with different characteristic impedances but a single propagation velocity, this fact implies that the per-unit-length (PUL) inductances can be calculated from the PUL capacitances for the homogeneous case [6].

Various analyses for coupled lines embedded in inhomogeneous medium have also been reported [1]–[9]. Tripathi performed a quasi-TEM analysis of symmetric coupled lines based on the structure's PUL impedance and admittance matrices [5]. Nguyen and Chang specialized this to the lossless case, where the impedance matrix becomes $j\omega[\mathbf{L}]$ and the admittance matrix becomes $j\omega[\mathbf{C}]$ [4]. Farina and others in paper [8] derive a coupled lines model from the "spot frequency" characteristics of transmission media derived by means of a numerical electromagnetic simulator. Levy uses a method of equivalent circuits for modeling the coupled lines [9].

In this paper, we present a detailed investigation of the model of coupled suspended striplines and microstriplines based on the moment method and partial charge images technique. We also report the results of its analysis.

Mathematical model of the microstrip coupled lines

In general case, electromagnetic waves of various configurations propagate in microstrip lines at various phase velocities. However influence of longitudinal electromagnetic field components on general wave configuration can be neglected in wide frequency range. Thus quasi-TEM approach can be used in the analysis of coupled microstrip lines.

TEM waves in coupled lines are named in accordance with relation of conductors widths. In case of equal widths, electromagnetic waves can be either even-mode or odd-mode. Even-mode wave propagates in lines if voltages equal in magnitude and sign are applied to the signal strips. Odd-mode wave propagates in case voltages equal in magnitude and opposite in sign are applied.

If widths of signal strips are unequal, TEM waves are called c-mode and out p-mode according to line excitation mode. It should be noted, that in case of unequal widths, voltages of signal strips can be different in sign and magnitude. Relation of voltages in case of c-mode and p-mode is denoted R_c and R_p respectively.

It is considered, that length of lines is infinite, and quasi-TEM waves propagate in lines. Thus, static analysis of cross-section of coupled microstrip line is enough to determine line parameters (Fig. 1).

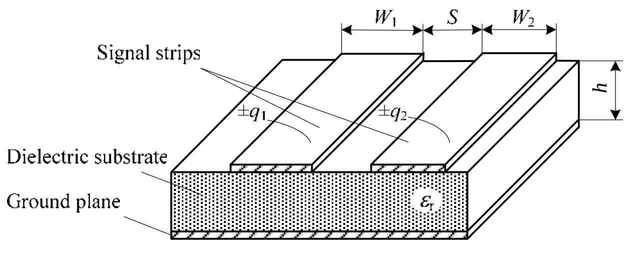

Fig. 1. Cross-section of coupled microstrip line

The main parameters of coupled microstrip lines: characteristic impedance of signal strips $Z_{1,2,c,p}$, effective relative dielectric permittivity $\varepsilon_{\mathrm{r\,eff}\,c,\pi}$, relation of voltages $R_{c,p}$ are found from capacitances of conductors [10]:

$$Z_{1c,\pi}=\left[c_0\sqrt{\left(C_{11}^a-R_{c,\pi}C_{12}^a\right)\left(C_{11}-R_{c,\pi}C_{12}\right)}\right]^{-1}, \quad (1)$$

$$Z_{2c,\pi}=\left[c_0\sqrt{\left(C_{22}^a-C_{12}^a/R_{c,\pi}\right)\left(C_{22}-C_{12}/R_{c,\pi}\right)}\right]^{-1}. \quad (2)$$

$$e_{\mathrm{r\ ef}\,c,p} = \frac{C_{11} - R_{c,p}C_{12}}{C_{11}^{a} - R_{c,p}C_{12}^{a}} = \frac{C_{22} - \left(C_{12}/R_{c,p}\right)}{C_{22}^{a} - \left(C_{12}^{a}/R_{c,p}\right)}; \qquad (3)$$

where subscripts 1 and 2 denote conductors, widths of which are W_1 and W_2 respectively; c and p subscripts denote of c-mode and p-mode; superscript a denotes capacitances of coupled microstrip line with same geometric properties but with no dielectric substrate (dielectric substrate is replaced with air).

Self capacitances C_{11}, C_{22}, C_{11}^{a}, C_{22}^{a} and mutual capacitances C_{12}, C_{12}^{a} are calculated by introducing so called *magnetic* and *electric* walls to the coupled microstrip line [11] or, in other words exciting signal strips in phase and out of phase respectively:

$$C_{11} = \left(C_{1o} + C_{1e}\right)/2\,; \quad C_{22} = \left(C_{2o} + C_{2e}\right)/2\,; \qquad (4), (5)$$

$$C_{12} = \left(C_{1o} - C_{1e}\right)/2 = C_{21} = \left(C_{2o} - C_{2e}\right)/2\,; \qquad (6)$$

$$C_{11}^{a} = \left(C_{1o}^{a} + C_{1e}^{a}\right)/2\,; \quad C_{22}^{a} = \left(C_{2o}^{a} + C_{2e}^{a}\right)/2\,; \qquad (7), (8)$$

$$C_{12}^{a} = C_{21}^{a} = \left(C_{1o}^{a} - C_{1e}^{a}\right)/2 = \left(C_{2o}^{a} - C_{2e}^{a}\right)/2\,; \qquad (9)$$

where C_{1e} and C_{2e} – capacitances per unit length of signal strips with widths W_1 and W_2 respectively, when magnetic wall is introduced to the system (or when voltages of same sign are applied to the strips); C_{1o}, C_{2o} – capacitances of the same signal strips, when electric wall is introduced (or voltages different in sign are applied); superscript a denotes capacitance calculated when dielectric substrate is replaced with air.

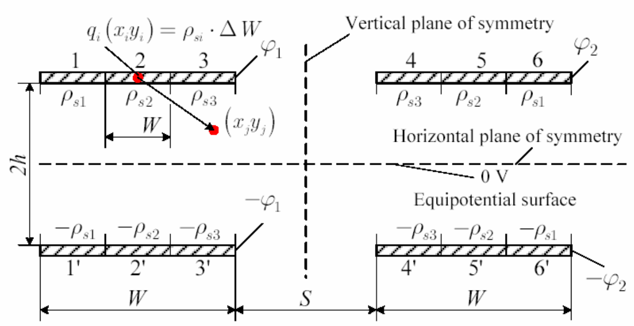

Fig. 2. Model of coupled microstrip lines in a homogeneous dielectric medium

Several methods can be used to determine capacitances, used in expressions (4)–(9). Among these are: conformal mapping [12]–[14], finite difference [15]–[17], finite elements [18], [19], spectral domain [20], [21], FDTD [22] etc. In model, investigated in this article, capacitances $C_{1,2,e,o}$ and $C_{1,2,e,o}^{a}$ are calculated using moment method [23]. This method is distinguished for it‘s low demands for computational resources in comparison with other methods.

Using the moment method, charge of the conductor is determined when voltage of the conductor is known. In this case capacitance is calculated by well known relationship $C = Q/j$, where Q – charge accumulated in the conductor and j – conductor voltage.

Model of coupled lines in a homogeneous dielectric

Applying the moment method, conductors in the cross section of coupled lines are divided into N equal sub-strips ΔW in width. Consider the model of coupled lines presented in Fig. 2. Conductors are divided into $N = 6$ sub-strips. It is assumed, that in every sub-strip i, charge is distributed uniformly with charge density r_{si}. For sake of simplicity, it is assumed, that charge of every sub-strip is concentrated in the string of infinitesimal thickness positioned in the center of the sub-strip, and charge per unit length of the sub strip is expressed by:

$$q_i = \rho_{si} \times \Delta W\,. \qquad (10)$$

Ground plane is modeled by introducing mirror pair of conductors with respect to ground plane, and applied opposite voltage, positioned at a distance $2h$ from the "real" pair of conductors (Fig. 2).

Charge at point P_i and its potential, created in point P_j are related by Green's functions [24]:

$$G(P_i : P_i) = -\frac{1}{2\pi\varepsilon}\left[\ln\left(\frac{\Delta W}{2}\right) - 1\right], \qquad (11)$$

$$G(P_j : P_i) = -\frac{1}{2\pi\varepsilon}\ln R(P_j : P_i), \qquad (12)$$

where $P_i : P_i$ denotes charge at point P_i and its created potential at the same point; $P_j : P_i$ denotes charge and its created potential at different points P_j and P_i; $R(P_j : P_i)$ – distance between points P_j and P_i. In case points P_i and P_j are in the same signal strip, $R(P_j : P_i) = |i - j|\Delta W$, if points are in different strips – $R(P_j : P_i) = |i - j|\Delta W + S$, where S is gap width between the strips.

According to the superposition principle, voltage at any point P_i is the sum of voltages, created by charges q_i positioned in all points P_j of the cross section of a coupled microstrip line:

$$q_i \equiv \sum_{j=1}^{N} G(P_j : P_i) + \sum_{j'=1}^{N'} G(P_j : P_i),$$
$$\text{when } 1 \le i \le N, \qquad (13)$$

where $\sum_{j=1}^{N} G(P_j : P_i)$ – Greens function, which expresses potential at point P_i in terms of positive charge accumulated in point P_j; $\sum_{j=1'}^{N'} G(P_j : P_i)$ – Greens function, which expresses potential at point P_i in terms of negative charge accumulated in point P_j. Green's functions in (13) are calculated using equations (11) and (12).

Charges accumulated in conducting strips are determined by solving linear equation system, which in matrix form can be expressed as:

$$[\varphi]=[\mathbf{G}]\times[\mathbf{q}], \qquad (14)$$

where $[\varphi]$ – column-matrix consisting of $2N$ elements of known potentials; $[\mathbf{G}]$ – $2N\times 2N$ matrix of Green's functions; $[\mathbf{q}]$ – column-matrix consisting of $2N$ elements of charges to be found. Equation system (14) can be solved by any conventional technique, e.g. by calculating inverse matrix of Green's functions and multiplying it by column–matrix of voltages:

$$[\mathbf{q}]=[\mathbf{G}]^{-1}\times[\varphi]. \qquad (15)$$

It should be noted, that in case of equal strip widths two planes of symmetry exist in the cross-section of a coupled lines (Fig. 2), therefore number of unknown charges reduces four times. In case widths are different, only horizontal plane of symmetry is present, and number of unknown elements is N .

Model of coupled lines in a non-homogeneous dielectric medium

In order to model coupled lines in a non-homogeneous dielectric medium, technique described in [24] shall be used. This technique is based on the principle of partial charge images [25]. According to this technique, influence on potential of point P_j (see Fig. 3) of every charge q_i is expressed in 6 steps:

1. Potential at point P_j created by the charge of the same point q_j and it's first partial image Kq_j is expressed by:

$$\varphi(P_j:P_j)=-\frac{(1+K)q_i}{2\pi\varepsilon_0}\left[\ln\left(\frac{\Delta W}{2}\right)-1\right], \qquad (16)$$

where $K=-\frac{\varepsilon_r-1}{\varepsilon_r+1}$ – reflection coefficient, ε_0 – dielectric constant.

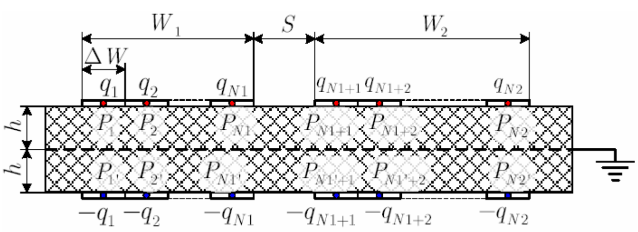

Fig. 3. Cross-section of couled microstrip line model in a non-homogeneous dielectric medium

2. Potential at point P_j created by all remaining charges of q_j is expressed by:

$$\varphi(P_j:P_j)=\frac{K(1-K^2)q_j}{2\pi\varepsilon_0}\sum_{n=1}^{\infty}K^{2(n-1)}\ln(4nh). \qquad (17)$$

3. Potential at point P_j, created by mirror charge $-q_j$ and all it's partial images is expressed by:

$$\varphi(P_j:P_{j'})=\frac{K(1-K^2)q_j}{2\pi\varepsilon_0}\sum_{n=1}^{\infty}K^{2(n-1)}\ln[(4n-2)h]. \qquad (18)$$

4. Potential at point P_j, created by charges q_i situated in all points P_i ($1\le i\le N$ and $i\ne j$, where $N = N1+N2$ – number of all unknown charges), and their first partial images Kq_j is expressed by:

$$\varphi(P_j:P_i)=-\frac{(1-K^2)q_i}{2\pi\varepsilon_0}\ln R(P_j:P_i). \qquad (19)$$

5. Potential at point P_j, created by all reaming partial charges of q_i situated in all points P_i, is expressed by:

$$\varphi(P_j:P_i)=\frac{K(1-K^2)q_i}{4\pi\varepsilon_0}\times$$

$$\times\sum_{n=1}^{\infty}K^{2(n-1)}\ln\left\{R(P_j:P_i)^2+(4nh)^2\right\} \qquad (20)$$

6. Potential at point P_j, created by mirror charges $-q_i$ at points $P_{i'}$ and all their partial images is expressed by:

$$\varphi(P_j:P_{2N-j+1})=\frac{(1-K^2)q_j}{4\pi\varepsilon_0}\times$$

$$\times\sum_{n=1}^{\infty}K^{2(n-1)}\ln\left\{R(P_j:P_i)^2+[(2n-1)2h]^2\right\}. \qquad (21)$$

Full potential at point P_j is expressed by summing all components of potential at that point. Expressions of full potentials of all points are found and equation system is built. In case potentials of both strips are equal to 1 V , equation system takes shape:

$$\begin{cases} 1= & G_{11}q_1+G_{12}q_2+ & \dots & +G_{1\frac{N}{2}}q_{\frac{N}{2}} \\ 1= & G_{21}q_1+G_{22}q_2+ & \dots & +G_{2\frac{N}{2}}q_{\frac{N}{2}} \\ \dots & \dots & \dots & \dots \\ 1= & G_{\frac{N}{2}1}q_1+G_{\frac{N}{2}2}q_2+ & \dots & +G_{\frac{N}{2}\frac{N}{2}}q_{\frac{N}{2}} \end{cases}, \qquad (22)$$

or in matrix form:

$$[\mathbf{1}]=[\mathbf{G}]\times[\mathbf{q}]. \qquad (23)$$

Coefficients G_{ij} define potential at point P_i created by charge q_j in expression (22). In case under consideration, coefficients G_{ij} are expressed by adding potentials, expressed by (16)–(21), and dividing by charge q_j :

$$G_{ij}=\sum_{j=1}^{6}\varphi(P_i:P_j). \qquad (24)$$

Column-matrix of unknown charges is calculated by solving linear equation system:

$$[\mathbf{q}] = [\mathbf{G}]^{-1} \times [\mathbf{1}]. \tag{25}$$

Capacitances per unit length of conducting strips are determined by summing all unit length charges of sub-strips:

$$C_{1e} = \sum_{i=1}^{N1} q_i\ , \quad C_{2e} = \sum_{i=N1+1}^{N2} q_i\ . \tag{26}$$

In case of odd mode wave propagation, elements of respective conductor strips in potential matrix are changed to - 1 . Further calculation procedure remains the same as for even mode wave propagation.
Characteristic impedances and effective relative dielectric permittivity are calculated by (1)–(3).

Results of investigation of the coupled lines model

Software tools have been developed by authors according to expressions (1)–(9) and (16)–(26). Normal mode parameters of symmetrically and asymmetrically coupled lines were calculated given various widths of gap between the strips and relations of strip widths. Calculation results were compared with published results worked out by other methods.

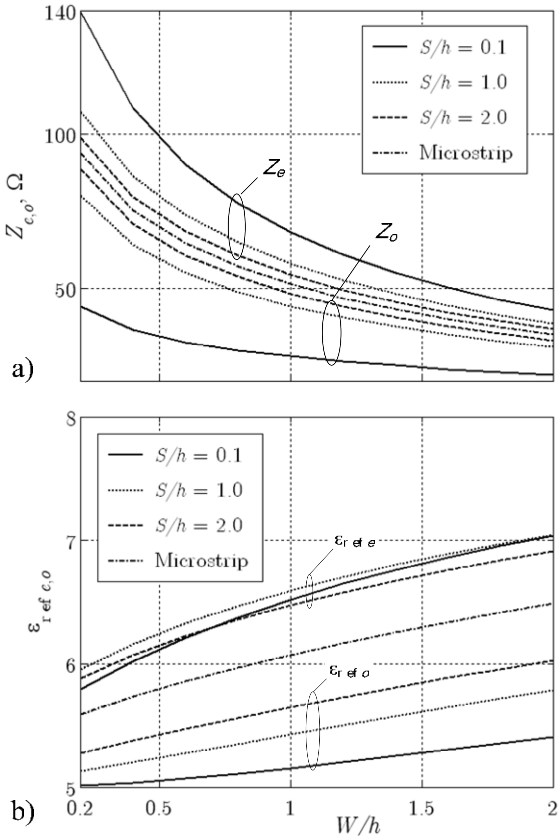

Fig. 4. Characteristic impedance (a) and effective dielectric constant (b) of coupled microstrip lines versus strip width and space between them. $\varepsilon_r = 9.6$

Dependence of characteristic impedance and relative effective permittivity on width of strips and gap width is presented in Fig. 4. It is seen that characteristic impedance decreases, and effective relative permittivity increases when width of strips increases for both – odd and even wave. Capacity per unit length of wider strips is higher, and more charge is accumulated in middle part of wider strips. This explains the dependencies presented in Fig. 4. Capacitance per unit length when even-mode wave propagates is lower than that when odd-mode wave propagates. Hence characteristic impedance and effective relative permittivity in case of even-mode are always higher than in case of odd-mode. Strength of electric field in the gap between the strips is much higher in case of odd-mode, than in case of even-mode; therefore charge density at the inner edges of strips is higher for odd-mode. On the other hand, majority of electric field lines is concentrated in the air between the strips; consequently effective relative permittivity is lower for odd-mode.

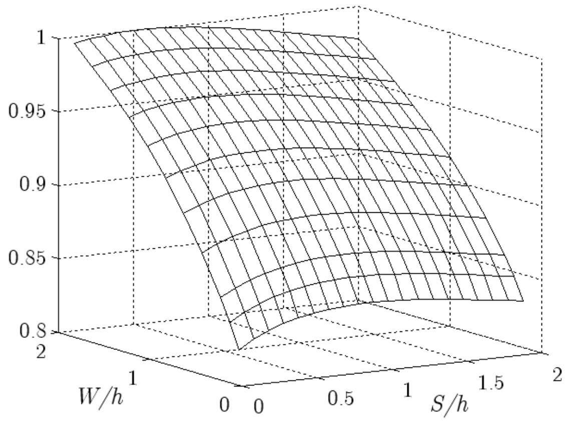

Fig. 5. Normalized relative effective dielectric constant of coupled microstrip lines as a function of strip width and space between them. $\varepsilon_r = 9.6$

It is known that, when gap between the strips decreases, interaction between the strips increases – electric field strength for odd-mode increases (charge at inner edges of strips increases), and field strength decreases in case of even-mode (charge at inner edges of strips decreases). Accordingly, when gap between the strips decreases, characteristic impedance increases for even-mode, and decreases in case of odd-mode. Dependence of effective relative permittivity on gap width for odd-mode is similar. In case of even-mode, dependence of effective relative permittivity on gap width is more complex. When gap width increases (and widths of strips remain constant), effective relative permittivity initially increases, and for higher values of gap width decreases (Fig. 5). This phenomenon is caused by changing of charge distribution at the inner and outer edges, and in middle parts of strips at the increase of gap width. When gap between strips increases (S/h is close to zero), charge density at outer edges of strips decreases, and less electric field lines cross air, thus effective relative permittivity increases. Further increase of gap width causes increase of charges at inner edges of strips; this in turn causes increase of electric field lines in air at the gap between strips. Therefore, effective relative permittivity decreases. It should be noted, that parameters of thinner strips are more sensitive to the change of gap width. This is due to higher

Table 1. Values of characteristic impedance of asymmetrically coupled lines calculated by various methods, when $W_1/W_2 = 0.6/1.2$, $h = 0.62$ mm, and $\varepsilon_r = 9.7$

S, mm	Reference [27]				Reference [26]				This method			
	Z_{c1}, Ω	Z_{c2}, Ω	$Z_{\pi1}$, Ω	$Z_{\pi2}$, Ω	Z_{c1}, Ω	Z_{c2}, Ω	$Z_{\pi1}$, Ω	$Z_{\pi2}$, Ω	Z_{c1}, Ω	Z_{c2}, Ω	$Z_{\pi1}$, Ω	$Z_{\pi2}$, Ω
0,1	74,50	42,15	34,45	19,49	75,50	43,90	35,00	20,70	72,78	42,48	34,63	20,21
0,2	70,81	41,50	38,85	22,77	71,43	42,86	39,64	24,30	69,57	41,61	39,10	23,39
0,3	68,04	40,90	41,58	25,05	68,57	42,14	42,82	26,43	67,02	40,85	41,89	25,53
0,4	65,90	40,40	43,51	26,69	66,43	41,43	44,29	27,86	64,96	40,18	43,87	27,14
0,5	64,28	40,01	44,96	27,99	64,29	40,71	46,43	29,29	63,29	39,62	45,34	28,38
0,6	62,99	39,67	46,10	29,04	63,21	40,00	47,50	30,35	61,91	39,13	46,48	29,38

relation between charges accumulated in edges of strips and in middle part of strips for thinner strips than for wider ones.

At the increase of gap width, interaction between strips decreases. It is seen in Fig. 4 that when ratio S / h increases, parameters of coupled lines approach to parameters of single microstrip line.

Comparison of characteristic impedance of coupled lines with same geometrical parameters determined by conformal mapping and spectral domain methods is presented in Table 1. It is seen that values of coupled lines characteristic impedance, determined by method under consideration is almost always a bit lower than values calculated by other methods (except characteristic impedance of the wider strip in out of phase mode). Nevertheless, relative error in respect of conformal mapping method is below 3.7%, and in respect of spectral domain method – below 3.8%. It must be noted, that values of characteristic impedance published in [26] are determined assuming signal of 10 GHz acts on a line, whereas influence of frequency is neglected in the model under consideration.

Conclusions

A model have been presented for calculating the quasi-static TEM design parameters of coupled transmission lines in an inhomogenous medium. Comprehensive comparisons between the results which are obtained by using the created model on one hand, and those obtained by a rigorous conformal mapping and spectral-domain analysis on the other hand, have shown an excellent accuracy of better than four percent for most of the practical ranges of physical dimensions. The model presented here are about 200 times faster than the finite difference analysis, hence it is especially applicable in CAD of (M)MIC design.

References

1. **Tsai L.-C., Chen H.-M., Hsue C.-W.** Z-domain formulations of equal-length coupled-serial-shunted lines and their applications to filters // IEE Proc. – Microw. Antennas Propag. – April 2004. – Vol. 151, No. 2. – P. 97–103.
2. **Pieters P., Brebels S., Beyne E., Mertens R.P.** Generalized analysis of coupled lines in multilayer microwave MCM-D technology–Application: Integrated coplanar Lange couplers // IEEE Transactions on MTT. – 1999. – Vol. 47, No. 9. – P. 1863–1872.
3. **Leong Y.C., Weinreb S.** Novel technique of phase velocity equalization for microstrip coupled-line phase shifters // IEEE MTT-S Dogest. – 2000. – Vol. TH2B-5. – P. 1453–1456.
4. **Nguen C., Chang K.** On the analysis and design of spurline bandstop filters // IEEE Transactions on MTT. – 1985. – Vol. 33, No. 12. – P. 1416–1421.
5. **Tripathi V. K.** Asymmetric coupled transmission lines in an inhomogeneous medium // IEEE Transactions on MTT. – 1975. – Vol. 23, No. 9. – P. 734–739.
6. **Marx K. D.** Propagation modes, equivalent circuits, and characteristic terminations for multiconductor transmission lines with inhomogeneous dielectrics // IEEE Transactions on MTT. – 1973. – Vol. 21, No. 7. – P. 450–457.
7. **Schwindt R., Nguyen C.** Spectral domain analysis of three symmetric coupled lines and application to a new bandpass filter // IEEE Transactions on MTT. – 1994. – Vol. 42, No. 7. – P. 1183–1188.
8. **Farina M., Morini A., Rozzi T.** On the derivation of coupled-line models from EM simulators and application to MoM analysis // IEEE Transactions on MTT. – 2005. – Vol. 53, No. 11. – P. 3272–3280.
9. **Levy R.** New equivalent circuits for inhomogeneous coupled lines with synthesis Applications // IEEE Transactions on MTT. – 1988. – Vol. 36, No. 6. – P. 1087–1094.
10. **Kundrotas A.**, **Martavičius R.**, **Urbanavičius V.**. Daugialaidės linijos su skirtingo pločio laidininkais modelis // Radioelektronika: Mokslo darbai. – 1994. – T. 30, Nr. 3. – P. 12–29.
11. **Martavičius R., Urbanavičius V.** Dviekranės daugialaidės linijos modelis // Elektronika ir elektrotechnika. – 1995. – Nr. 3. – P. 60–69.
12. **Штарас С**, **Станкунас Й**. Частотные свойства спиральных отклоняющих систем // Техника средств связи: Радиоизмерительная техника. – 1985. – Вып. 3. – С. 79–95.
13. **Gevorgian S., Berg H.** Line capacitance and impedance of coplanar-strip waveguides on substrates with multiple dielectric layers // Gallium Arsenide applications symposium. GAAS 2001. – London, 24-28 September 2001.
14. **Goano M., Bertazzi F., Caravelli P., Ghione G., Driscoll T. A.** A General Conformal-Mapping Approach to the Optimum Electrode Design of Coplanar Waveguides With Arbitrary Cross Section // IEEE Transactions on Microwave Theory and Techniques. – September 2001. – Vol. 49, No. 9. – P. 1573–1580.
15. **Martavičius R., Urbanavičius V.** Metodika nepastovaus žingsnio daugialaidės linijos ilginėms talpoms apskaičiuoti // Elektronika ir elektrotechnika. – Kaunas: Technologija, 2002. – Nr. 6 (41). – P. 47–53.
16. **Kleiza A., Štaras S.** Daugialaidžių linijų banginių varžų skaičiavimas // Elektronika ir elektrotechnika. – Kaunas: Technologija, 1999. – Nr. 4 (22). – P. 41–44.
17. **Bondeson A., Rylander T., Ingelström P.** Computational Electromagnetics // Texts in Applied Mathematics. Volume 51. Springer Berlin Heidelberg. ISBN: 978-0-387-26158-4. – 2006. – P. 19–35.
18. **Huebner K. H., Dewhirst D. L., Smith D. S., Byrom T. G.** The Finite Element Method for Engineers. – Wiley-Interscience. ISBN-10: 0471370789. – 2001. – 744 p.

19. **Bondeson A., Rylander T., Ingelström P.** Computational Electromagnetics / Texts in Applied Mathematics. Volume 51. Springer Berlin Heidelberg. ISBN: 978-0-387-26158-4. – 2006. – P. 87–151.
20. **Pannier P., Kadri L., Seguinot C., Kennis P., Huret F.** Accurate and efficient numerical method for the analysis of multimode waveguide discontinuities // IEEE Transactions on MTT. – 2000. – Vol. 48, No. 2. – P. 295–304.
21. **Gentili G. G., Salazar-Palma M.** The definition and computation of modal characteristic impedance in quasi-TEM coupled transmission lines // IEEE Transactions on MTT. – 1995. – Vol. 43, No. 1. – P. 338–343.
22. **Liou L. L., Mah M. Y., Ferendeci A.** Equivalent circuit parameter extraction of microstrip coupling lines using FDTD method // IEEE Antennas and Propagation Society International Symposium, 2000. – 16–21 July 2000. – Vol. 3. – P. 1488–1491.
23. **Harrington R. F.** Field Computation by Moment Methods / New York: IEEE Press, 1993. – 229 p.
24. **Urbanavičius V., Martavičius R**. Model of the microstrip line with a non-uniform dielectric // Electronics and Electrical Engineering. – Kaunas: Technologija, 2006. – Nr. 3 (67). – P. 55–60.
25. **Silvester P. P., Ferrari R. L.** Finite Elements for Electrical Engineers / Cambridge, UK: Cambridge University Press, 1996. – 512 p.
26. **Janhsen A., Hansen V.** Determination of the Characteristic Impedance of Single and Coupled Lines in Layered Dielectric Media // Microwave Symposium Digest, 1991, IEEE MTT-S International, Boston, MA. – 10-14 June 1991. – INSPEC Accession Number: 4086527. – Vol.2. – P. 765–768.
27. **Bedair S. S.** Characteristics of some asymmetrical coupled transmisssion lines // IEEE Trans. On MTT. – 1984. – Vol. MTT-32, No. 1. – P. 108–110.

Submitted for publication 2007 03 01

V. Urbanavičius, Š. Mikučionis, R. Martavičius. Model of the Coupled Transmission Lines with a non-uniform Dielectric // Electronics and Electrical Engineering. – Kaunas: Technologija, 2007. – No. 5(77). – P. 23–28.

The mathematical model of the coupled transmission line (CTL) with non-uniform dielectric in its cross-section is presented in the article. Supposed mathematical model is created using the method of moments and the technique of partial images of the charges. The created model allowed us to determine the charge distribution on the signal conductors, capacitances per unit length, and characteristic impedances of the CPL, when even-, odd-, c- or π-modes are excited in them. The accuracy of supposed model was verified using the software which was created by authors. In this article the authors investigated electrodynamical characteristics of CTLs when it sizes and the substrate permittivity were changed in a wide range. A comparison of the calculated characteristics of author's model with the results from other articles showed that they coincided. Ill. 5, bibl. 27 (in English; summaries in English, Russian and Lithuanian).

В. Урбанавичюс, Ш. Микучионис, Р. Мартавичюс. Модель связанных линий передачи, учитывающая неоднородность диэлектрика // Электроника и электротехника. – Каунас: Технология, 2007. – № 5(77) – С. 23–28.

Представлена математическая модель связанных линий передачи (СЛП) учитывающая неоднородность диэлекрика в поперечном сечении линии. Для построения математической модели использован метод моментов и принцип частичных отражений зарядов. Созданная модель позволяет установить распределение заряда на сигнальных проводниках линии, а также рассчитать погонную ёмкость и характеристический импеданс сигнальных проводников анализируемой СЛП при распространении в ней четных, нечетных, синфазных или противофазных нормальных волн. Точность созданной математической модели проверялась авторами с помощью написанного ими программного обеспечения. Были рассчитаны электродинамические параметры СЛП в широком интервале изменения конструктивных параметров линии. Проведённые расчёты показали хорошее совпадение получаемых результатов с публикуемыми в научной литературе. Ил. 5, библ. 27 (на английском языке; рефераты на английском, русском и литовском яз.).

V. Urbanavičius, Š. Mikučionis, R. Martavičius. Susietųjų perdavimo linijų modelis dielektriko nevienalytiškumui įvertinti // Elektronika ir elektrotechnika. – Kaunas: Technologija, 2007. – Nr. 5(77). – P. 23–28.

Pateiktas susietųjų perdavimo linijų matematinis modelis, įvertinantis dielektriko nevienalytiškumą linijos skerspjūvyje. Matematiniam modeliui sudaryti pritaikytas momentų metodas ir krūvių dalinių atvaizdų principas. Sukurtas matematinis modelis leidžia nustatyti elektros krūvio pasiskirstymą signalinių laidininkų skerspjūvyje, taip pat apskaičiuoti analizuojamų susietųjų linijų laidininkų ilgines talpas ir būdinguosius impedansus esant lyginiam, nelyginiam, sinfaziniam ar priešfaziniam jų sažadinimui. Siūlomo modelio tikslumas patikrintas autorių sukurta programine įranga. Skaičiavimų rezultatai gerai sutampa su publikuotais mokslinėje spaudoje, esant plačiam analizuojamų susietųjų linijų konstrukcinių parametrų ruožui. Il. 5, bibl. 27 (anglų kalba; santraukos anglų, rusų ir lietuvių k.).